A quiescent state following mild sensory arousal in *Caenorhabditis elegans* is potentiated by stress

Patrick D. McClanahan[1], Jessica M. Dubuque[1], Daphne Kontogiorgos-Heintz[1], Ben F. Habermeyer[1], Joyce H. Xu[1], Anthony M. Ma[1], David M. Raizen[2], Christopher Fang-Yen[1,3]

[1]Department of Bioengineering, University of Pennsylvania School of Engineering and Applied Science, Philadelphia, PA, USA, [2]Department of Neurology, University of Pennsylvania School of Medicine, [3]Department of Neuroscience, University of Pennsylvania School of Medicine

Correspondence should be addressed to P.D.M. (email: pdmcclanahan@gmail.com) or C.F.-Y. (email: fangyen@seas.upenn.edu)

Author contributions: PDM performed experiments and wrote the manuscript, JMD, DKH, BFH, JHX, and AM performed experiments, DMR provided scientific guidance, and CFY supervised the project and edited the manuscript.

Abstract

In response to threats, animals display quiescent behaviors such as freezing and tonic immobility. How neuromodulatory states like stress affect these behaviors is not well understood. Here we describe a *Caenorhabditis elegans* quiescent behavior, post-response quiescence (PRQ), which is modulated by the *C. elegans* response to cellular stressors. Following an aversive mechanical or blue light stimulus, worms respond first by briefly moving, and then become more quiescent for a period lasting tens of seconds. PRQ occurs at low frequency in unstressed animals, but is more frequent in animals that have experienced cellular stress due to ultraviolet light exposure as well as in animals following overexpression of epidermal growth factor (EGF). PRQ requires the function of the carboxypeptidase EGL-21 and the calcium-activated protein for secretion (CAPS) UNC-31, suggesting it has a neuropeptidergic mechanism. Although PRQ requires the sleep-promoting neurons RIS and ALA, it is not accompanied by decreased arousability, and is not homeostatically regulated, suggesting that it is not a sleep state. PRQ represents a simple, tractable model for studying how neuromodulatory states alter behavioral responses to stimuli.

Introduction

Quiescent animal behaviors encompass low-vigilance states like sleep[1] and hibernation[2], but also include high-vigilance states that play important roles in the threat response[3,4]. The mammalian response to predatory threats includes four behaviors: freeze, flight, fight, and tonic immobility[5]. Animals freeze upon detecting a relatively distant threat in order to reduce conspicuousness while preparing for the next two stages: flight or fight[3,6] , which

are active behaviors occurring at intermediate to close range. Tonic immobility typically occurs once a prey animal is very near to or in the grip of a predator. Tonically immobile animals may appear dead, but are in fact alert and able to escape if the predator becomes distracted or lets go[7]. Therefore, freezing and tonic immobility are quiescent behaviors with high vigilance.

The regulation of freezing and tonic immobility is intertwined with animals' physiological response to stress. In mammals, acute threats and stressors precipitate the release of epinephrine (adrenaline) and norepinephrine (noradrenaline), increasing muscle tone and cardiac output to prepare for fight or flight[3]. This sympathetic nervous system activation is also the first phase of the general stress response, or *general adaptation syndrome*[8]. The transient alarm phase is followed by a much longer resistance phase[9] in which glucocorticoids like cortisone are elevated. These hormones have many functions, including mobilizing energy stores, and they upregulate both freezing[3] and tonic immobility[10]. The resistance phase typically ends with either exhaustion or removal of the stressor, but upregulation of threat responses following stress can persist as observed in psychological disorders including post-traumatic stress disorder[11]. Despite its significant medical and public health implications, our understanding of the regulation of threat response behavior by stress remains quite limited[12].

The study of genetically tractable models can increase our understanding of the regulation of behavior. Like mammals, the nematode *Caenorhabditis elegans* has a stereotypical response to stressors. Following exposure to a stressor like heat or UV radiation, the worm exhibits a period of quiescence[13] that aids survival[14–16]. This quiescence is mediated by the ALA and RIS neurons, which can be activated by the EGF homologue LIN-3[16], releasing a cocktail of neuropeptides, including those encoded by *flp-13*[17,18]. Like sleep, this recovery quiescence is associated with reduced responsiveness to some stimuli[14,19], but the quiescence can be rapidly reversed by a sufficiently strong stimulus[14]. Quiescence after stress is therefore similar to recovery sleep or quiescence in response to illness or injury in other animals and is referred to as stress-induced sleep (SIS)[20]. In mammals, EGF signaling promotes behavioral quiescence and sleep[21,22] and is released following stress[23], suggesting a conserved role in animal stress response regulation.

Like its stress response, the *C. elegans* acute escape behavior following threatening stimuli has been extensively characterized. Six touch-receptor neurons sense gentle mechanical stimuli to the body as well as substrate vibration, allowing the animal to quickly accelerate forward or backward away from the stimulus[24,25]. Similar behavioral responses occur following aversive chemical[26], osmotic[27], photic[28], and thermal[29] stimuli. In invertebrates, tyramine and octopamine function analogously to epinephrine and norepinephrine in the fight or flight response[30,31], and the *C. elegans* locomotor escape response is accompanied by a tyramine-dependent[31] inhibition of side-to-side head movements[24]. Mutations that impair touch sensitivity or head movement suppression during backing increase the worm's susceptibility to predation by trap-forming *Drechslerella doedycoides* fungi[32]. However, little is known about how stress affects *C. elegans* escape behavior, and behaviors resembling freezing or tonic immobility have not been described.

Here we describe a freezing behavior following locomotor escape behavior after mild aversive stimuli. We show that this behavior, which we call post response quiescence (PRQ), is enhanced following the EGF-mediated cellular stress response. We find that some of the genes and neurons required for SIS are also required for PRQ. Like SIS, PRQ requires genes involved in the processing and secretion of neuropeptides, and the sleep active interneurons RIS and ALA. Despite its genetic and anatomical overlap with *C. elegans* sleep states, PRQ lacks two of the behavioral characteristics of sleep – decreased arousability and homeostatic regulation – suggesting it is distinct from sleep. The occurrence of PRQ during an escape response and upregulation by the stress response pathway suggest a role in predator evasion similar to freezing behavior in mammals.

Results

Quiescence increases after mechanosensory response during UV stress-induced sleep

We asked how cellular stress affects the *C. elegans* behavioral response to aversive mechanical stimuli. To induce SIS, we exposed young adult wild-type (WT) animals to UV radiation[33]. After the given exposure of UV irradiation, the animals became sterile and died within one week **(Supplementary Fig. S1)**, suggesting that they sustain considerable damage[33]. To track behavior, we imaged worms isolated in wells of a multi-well device (WorMotel)[34] and used frame subtraction[35] to measure behavioral activity and quiescence (see Methods). Consistent with previous reports, quiescence reached a maximum 1 – 2 hours following UV-C exposure then decreased over the next 5 hours **(Fig. 1a)**. The peak fraction of time spent quiescent was about 70%, allowing for the detection of both increases and decreases in quiescence.

To deliver mechanical stimuli, we attached a WorMotel containing the worms to an audio loudspeaker, which was driven by a computer and amplifier to produce 1 s duration, 1 kHz frequency vibrations every 15 minutes. Substrate vibrations elicit a mechanosensory response mediated by the gentle touch receptors[36,37]. Both chemosensory and photosensory responsiveness are known to decrease during SIS[14,33], and mechanosensory arousability decreases in another *C. elegans* sleep state, developmental lethargus[38,39]. Consistent with decreased overall sensory arousability, mechanosensory responses decreased during SIS relative to controls, displaying a minimum at the time of peak quiescence **(Fig. 1b)**.

Despite an overall decrease in activity during SIS, most worms usually showed movement in response to the mechanical stimulus. We noticed that UV-treated worms sometimes froze for short periods (tens of seconds) following their brief locomotor response **(Supplementary Vid. 1)**. Control animals, which had not been exposed to UV light, rarely displayed this freezing behavior, instead displaying normal mechanosensory responses **(Supplementary Vid. 2)**.

To quantify this freezing behavior, we compared the peak fraction of animals quiescent before and after the stimulus (see Methods). Significant increases in quiescence following mechanostimulus occurred after the time of deepest SIS, becoming statistically significant in the 2-4, 4-6, and 6-8 hour periods ($p = 0.032$, 0.007, and 0.001, respectively) **(Fig. 1a,c)**. We did not find a significant increase in quiescence in the first and second hours after UV exposure, or in control animals at any time **(Fig. 1a)**, although we occasionally observed similar behavior in untreated controls **(Supplementary Vid. 3)**. We refer to this behavior, a cessation of body movement following a mechanosensory response, as post-response quiescence (PRQ) **(Fig. 1d)**.

Together, these results suggest that UV stress affects mechanosensory response behavior in two ways. First, the overall locomotor activity following the stimulus is reduced, consistent with a lower arousability during SIS. Second, beginning about two hours after UV exposure, the animals freeze after initiation of an otherwise normal mechanosensory response, and before returning to baseline quiescence levels.

Post response quiescence is enhanced following LIN-3C / EGF overexpression.

SIS caused by UV and other stressors occurs following activation of the ALA neuron, and possibly the RIS neuron[16], by the EGF homologue LIN-3[13,14]. We therefore asked whether PRQ is regulated downstream of EGF, or is part of an EGF-independent UV stress response. To address this question, we induced overexpression of EGF by heating (33°C for 10 min) animals carrying a *lin-3c* transgene under the control of a heat shock promoter. In contrast to reported severe heat shock (35-37 °C for 30 min[14]), this mild heat shock paradigm had minimal effects on control animals that did not carry the hs:EGF transgene. As reported[13,33], LIN-3 overexpression caused an overall increase in quiescence and decrease in arousability with dynamics similar to that of UV SIS **(Fig. 2a,b)**. We then used our mechanostimulus protocol to study the mechanosensory response.

We found that PRQ occurs following EGF overexpression-induced quiescence, and resembles PRQ after UV exposure **(Fig. 2a,c)**. This result is consistent with PRQ being upregulated downstream or in parallel to EGF signaling during SIS. For our parameters for UV exposure and EGF overexpression, the increase in fraction quiescent following mechanostimulus was greater after EGF overexpression (reaching a maximum of 0.25 ± 0.07 in hours 4.5-7) than after UV exposure (reaching a maximum of 0.12 ± 0.06 in hours 4-6 after UV-C exposure **(Fig. 1a, 2a)**.

Post-response quiescence following mechanostimulus requires touch receptor neuron function

Though we expected that our mechanical vibration stimulus generated a response and

PRQ through the touch receptor neurons, it remained possible that vibration induced PRQ by a mechanism independent of these cells. To ascertain whether PRQ requires the function of the touch receptor neurons, we assayed for PRQ in EGF-overexpressing worms containing a *mec-4* mutation, which causes a defective behavioral response to vibration[24] **(Supplementary Fig. S2)**. EGF-overexpressing *mec-4* mutants had neither a movement response nor a PRQ response to the vibration. This result indicates that PRQ occurs downstream of activation of the touch receptor neurons and possibly the escape response that they mediate.

Post response quiescence is not enhanced following a variety of other cellular stressors.

In addition to UV radiation, exposure to ethanol, high salt, Cry5b pore-forming toxin, heat shock, and cold shock also induce SIS[14]. To test whether these stressors also promote PRQ, we assessed quiescence changes following vibration in animals exposed to these stressors. We compared the behavioral response to control animals on the same WorMotel chip (see Methods). Consistent with previous reports[14], we observed an increase in quiescence in animals exposed to these stressors **(Supplementary Fig. S3)**. However, we found to our surprise that in no case was PRQ significantly higher in SIS animals than in control animals that had not been exposed to the stressors **(Fig. 3)**. These results show that PRQ is enhanced by EGF signaling and by UV exposure, but is not strongly enhanced by a variety of cellular stressors that also cause SIS, suggesting that aspects of the general response to cellular stress depend on the type of stressor.

Post-response quiescence requires neuropeptide signaling and the sleep active neurons ALA and RIS.

We asked whether PRQ, a type of behavioral quiescence, depends on neurons required for other quiescent behavior. The sleep-active interneurons ALA[16] and RIS[40] regulate *C. elegans* behavioral quiescence. The homeodomain transcription factors CEH-14 and CEH-17 are required for proper differentiation of the ALA neuron[41], and loss of function of either of these genes causes a near total loss of EGF-quiescence[13,41]. Another transcription factor, APTF-1, is required for the quiescence-promoting function of RIS[40]. In *aptf*-1 mutants, movement quiescence during lethargus is severely curtailed[40,42]. The RIS neuron plays a role in several other forms of quiescence, including fasting quiescence, satiety quiescence, quiescence associated with early larval developmental diapause[43], and SIS[16].

To test whether ALA or RIS play a role in PRQ, we overexpressed EGF in *ceh-17, ceh-14,* or *aptf-1* backgrounds. EGF-induced quiescence was severely reduced in each of these mutants **(Fig. 4a, Supplementary Fig S4a)**. These results show that both ALA and RIS regulate EGF-induced quiescence, as previously reported[13,16].

Following mechanical stimulus 2-12 h after induction of EGF overexpression, neither

ceh-17 nor *aptf-1* mutants showed an increase in quiescence, suggesting that both ALA and RIS are required for PRQ. However, we observed a difference in the behavior of these mutants: *ceh-17* and *ceh-14* mutant animals showed a brief recovery of quiescence to baseline levels within the first minute after the mechanical stimulus, but this was followed by several minutes of reduced quiescence **(Fig. 4b,c, Supplementary Fig. S4b)**. In contrast, *aptf-1* mutants responded to the vibration by briefly moving and then gradually returning to baseline quiescence levels over the course of several minutes. As a result, *aptf-1* mutants had a significant *decrease* ($p = 0.0004$) in peak quiescence in the two minutes following the stimulus **(Fig. 4c)**.

ALA and RIS regulate sleep and quiescent behavior through the release of sleep-promoting neuropeptides, including those encoded by *flp-13*[17], *flp-24*, *nlp-8*[18] and *flp-11*[42], respectively. NLP-22, a neuropeptide expressed in the RIA interneuron, also promotes quiescence[44]. We therefore asked whether PRQ is also regulated by neuropeptide signaling. EGL-21 is a carboxypeptidase[45] required for the processing of members of both the FMRF-amide-like (FLP) and neuropeptide-like (NLP) neuropeptide families, and UNC-31 is the *C. elegans* homologue of the calcium-dependent activator protein for secretion (CAPS), which is required for dense core vesicle release[46]. To test whether neuropeptide signaling regulates PRQ, we studied animals overexpressing EGF in *egl-21* and in *unc-31* mutant backgrounds.

Mutants of *egl-21* and *unc-31* showed reduced EGF-induced quiescence compared to control animals overexpressing EGF in a wild-type background **(Supplementary Fig. S4)**. Following substrate vibration, the quiescence of *egl-21* mutants stayed below baseline levels for several minutes, similar to the observation in *aptf-1* mutants. *unc-31* mutants, while also lacking PRQ, quickly returned to baseline quiescence levels **(Supplementary Fig S4b)**. Because *unc-31* animals move sluggishly[47] and have reduced touch sensitivity (M. Chalfie, personal communication), we asked if a reduced movement response to mechanical stimuli might explain their lack of PRQ. To address this question, we restricted our comparison of PRQ to episodes in which *unc-31* mutants had a movement response to mechanical stimulus that was similar in magnitude to that of wild-type controls. We found that *unc-31* animals with mechanosensory response activity similar to that of WT animals were still defective in PRQ **(Supplementary Vid. 4, Figs. S5, S6)**.

In addition to expressing FLP-11, RIS also expresses markers of GABAergic neurons[42,48]. We first asked whether GABA signaling is required for SIS by measuring quiescence after UV exposure in *unc-25* mutants. The gene *unc-25* encodes a glutamate decarboxylase required for GABAergic neurotransmission[49]. Overall quiescence following EGF overexpression was similar between *unc-25* and wild-type controls **(Supplementary Fig. S7a)**. We asked whether GABA signaling plays a role in PRQ. *unc-25* mutants showed a decrease in PRQ as measured by change in peak quiescence, and a slight change in shape of the PRQ peak, suggesting that GABA plays a role in regulating the depth and dynamics of PRQ **(Supplementary Fig. S7b,c)**. This result suggests that the regulation of quiescence in response to stress and the regulation of PRQ are controlled by overlapping but distinct mechanisms.

These results show that PRQ is regulated by neuropeptide and GABA signaling and by the quiescence-promoting interneurons ALA and RIS.

Post response quiescence does not fulfill criteria for sleep or sleep homeostasis

Because PRQ requires some of the same neurons and genes as two previously described *C. elegans* sleep states (SIS and developmental-timed sleep, or lethargus) we wondered whether PRQ might also be a form of sleep. We performed several experiments to test this idea.

Homeostatic regulation is a characteristic of sleep[1,50]. Sleep homeostasis manifests as an increase in sleep or sleep drive in compensation for deprivation of sleep. In *C. elegans*, sleep consists of alternating bouts of activity and quiescence. Brief or prolonged interruption of these quiescent bouts can cause short[51,52] or long-term[35,53] homeostatic increases in quiescence, respectively. Because PRQ consists of a brief period of increased quiescence following the response to a transient stimulus, we asked whether PRQ is a short-term homeostatic rebound of SIS.

Short-term homeostasis during lethargus resembles PRQ behaviorally in that it consists of several minutes of increased quiescence following a brief (1 second) substrate vibration. This homeostatic compensation is associated with a positive correlation between the durations of quiescent bouts and the preceding active bout, even in the absence of experimental stimuli, a phenomenon that has been named microhomeostasis[51,52]. We reproduced these prior results, finding a significant ($p = 0.01$) positive correlation between the durations of quiescent and movement bouts during lethargus **(Fig. 5a)**.

We examined the bout architecture of UV SIS to determine if, like lethargus, it also exhibits microhomeostasis. During UV SIS, quiescent bout durations were not significantly correlated with the preceding movement bout duration **(Fig. 5a)**. There was a weak positive correlation between quiescent and movement bouts in EGF-induced quiescence, but this correlation did not reach statistical significance ($p = 0.089$ **(Supplementary Fig. S8)**. These results suggest that PRQ is distinct from short-termhomeostasis in that it is not associated with microhomeostasis.. While we sought to compare PRQ and short-term homeostasis directly, we were unable to replicate the increase in quiescence in L4 lethargus animals following mechanostimulus reported by Nagy *et al.*[52] **(Supplementary Fig. S9)**.

Next we asked whether PRQ might be a form of sleep homeostasis. In other animals, sleep duration and/or depth is proportional to the duration of prior wakefulness. If PRQ is a form of sleep homeostasis, then increasing the amount of quiescence interruption should increase the amount of PRQ. We performed several experiments to test this prediction. First, we induced EGF overexpression in WT-background animals and gave them aversive mechanosensory or photosensory stimuli every 15 minutes. Unlike in previous experiments, we varied the duration

of these stimuli. As expected, longer duration mechanosensory and photosensory stimuli caused a larger increase in activity. However, increased response magnitude was associated with a *decrease* rather than an increase in quiescence, suggesting that PRQ is not a homeostatic compensation for stimulus-evoked activity during a quiescent state **(Fig. 5b,c, Supplementary Fig. S10)**. Next, we examined responses to 1-second substrate vibrations. We compared the increase in quiescence in animals in which the stimulus occurred during a quiescent bout to that in animals in which the stimulus occurred during an active bout. If PRQ were explained by a homeostatic response to disruption of quiescence, then the PRQ magnitude should be larger in cases where vibration disrupted a bout of quiescence than in cases where vibration occurred during a movement bout. We did not observe a difference in PRQ between these groups ($p = 0.17$) **(Fig. 5d)**. These results suggest that PRQ is not a homeostatic compensation for interruption of quiescence.

Lastly, we sought to determine whether PRQ itself fulfills three additional behavioral criteria used to distinguish sleep from other quiescent states. These criteria are rapid reversibility, decreased response to stimuli, and homeostatic regulation[1,50]. To determine whether PRQ fulfills these criteria, we used a 1-second substrate vibration to induce PRQ, and then applied another 1 second substrate vibration 15 seconds later, at the peak of PRQ. PRQ animals responded to the second stimulus, indicating that PRQ is reversible. However, these animals showed a greater increase in activity after the second stimulus than after a single stimulus ($p = 0.028$), indicating that PRQ is not associated with decreased arousability. Furthermore, we did not observe a second PRQ peak following the second stimulus, suggesting that PRQ itself is not under homeostatic regulation **(Fig. 5e,f)**. Taken together, these results show that PRQ lacks two of the four behavioral criteria for sleep: reduced arousability and homeostatic regulation.

During PRQ, lateral head movements are suppressed during locomotor pauses

Quiescent states often involve the coordinated suppression of multiple behaviors. Different aspects of SIS quiescence – locomotion, head movement, feeding, and defecation – are regulated by different combinations of neuropeptides[18]. On the other hand, active behaviors can also involve inhibition of movements, such as in the suppression of side to side head movements during the escape response[32,54]. We asked how different types of behavioral quiescence may be coordinated during PRQ.

Our image subtraction-based analysis in the WorMotel could not distinguish between head movement and whole-body locomotion[55] or detect pharyngeal pumping, an indicator of feeding[56]. To assay these more subtle behaviors we recorded videos with higher spatial and temporal resolution of the mechanosensory responses of individual animals on agar pads before and after EGF induction. We then manually scored lateral head movements (including movements of only the nose), forward and reverse locomotion (mid-body movement relative to the substrate), and pharyngeal pumping.

We first sought to verify that EGF-induced quiescence and PRQ could be recapitulated in this agar pad preparation. Consistent with previous reports[13,18], EGF overexpression decreased overall locomotion, head movement, and pumping rate **(Supplementary Fig. S11)**. In our WorMotel analysis, quiescence is defined as lack of movement throughout the body, and therefore implies simultaneous quiescence in both locomotion and head movement. To compare our WorMotel data to our higher resolution agar pad data, we defined simultaneous locomotion and head movement quiescence as "body quiescence". We found a significant increase in body quiescence after the stimulus ($p = 0.015$) with a time dependence comparable to our WorMotel data for PRQ **(Fig. 6a,b)**. These results confirm that worms exhibit PRQ in our high-resolution assay.

Next, we examined the two components of body quiescence, head movement and locomotion quiescence. To our surprise, we observed no increase in locomotion quiescence after vibration in EGF induction animals, indicating that locomotion quiescence does not increase during PRQ. In contrast, we found a significant increase in head quiescence after mechanostimulus ($p = 0.007$) **(Fig. 6b)**, indicating that head movement, and not locomotion, is suppressed during PRQ.

If the timing of head movement quiescence and locomotion quiescence bouts was statistically independent, we would expect the product of the fractions of head movement and locomotion quiescence to be equal the fraction of body quiescence. In fact, we found that body quiescence fraction was greater than the product of the head movement quiescence and locomotion quiescence fractions. Indeed, beginning about 10 s after the mechanostimulus, head movement and body movement quiescence are at similar levels **(Fig. 6a)**. This observation suggests that during the timeframe of PRQ, head movement quiescence specifically occurs while the animal is undergoing locomotion quiescence. Consistent with this observation, comparison of the rate of head movement quiescence during forward, reverse, and pause locomotion states, before and after mechanostimulus, shows that head movement quiescence was greatest when the animal was pausing after mechanostimulus **(Fig. 6c)**.

Using our high-resolution assay, we also asked to what extent feeding is suppressed during PRQ. We found that pumping rate decreased after the mechanostimulus, consistent with findings that mechanosensory stimuli inhibit pumping[25,57]. However, the magnitude of decrease in pumping rate following mechanostimulus was similar before and after EGF induction **(Fig. 6d,e)**. This finding suggests that feeding behavior does not display an EGF-inducible quiescence following mechanostimulus similar to the suppression of body movement during PRQ.

These results suggest that during PRQ, locomotion and head movement quiescence are coordinated such that head quiescence occurs during locomotor pauses.

Discussion

In this study we have described PRQ, a form of quiescence that follows *C. elegans* responses to mild, aversive stimuli. This behavior is distinct from other forms of quiescence

previously described in *C. elegans*. For example, animals touched in the anterior part of the body will sometimes exhibit an immediate and brief pause in forward movement[58]. Compared to these pauses, PRQ is much longer in duration and occurs with a delay relative to the stimulus. As another example, animals confined to small spaces engage in long-term quiescent behavior[59]. PRQ occurs more quickly and is much shorter in duration than this confinement induced quiescence.

Several lines of evidence suggest that PRQ is related to SIS. PRQ is potentiated following UV SIS and following overexpression of EGF, which is thought to mediate the stress response, and PRQ and SIS share a dependence on the ALA and RIS quiescence-promoting interneurons and neuropeptide signaling. However, PRQ may not be a direct consequence of SIS, as some forms of stress induce SIS but not PRQ. Furthermore, the time course of PRQ following stress or EGF overexpression is distinct from that of SIS, with PRQ reaching a maximum after that of SIS and continuing many hours after cessation of the SIS response.

We asked what might be the adaptive significance of the PRQ behavior. Here we consider three ideas: (1) PRQ reflects a homeostatic mechanism in SIS (2) PRQ results from energy conservation, and (3) PRQ is a form of defensive freezing.

Given the association between PRQ and SIS, we first considered the possibility that PRQ represents a homeostatic mechanism in SIS. However, during PRQ, animals do not exhibit reduced arousability or homeostatic regulation, and therefore do not exhibit the properties expected for a homeostatic mechanism for sleep.

A second possible interpretation of PRQ is in terms of energy conservation. *C. elegans* locomotion requires energy expenditure[60], and cessation of feeding and activation of DNA repair pathways may contribute to reduced energy stores during UV SIS[61]. Indeed, fat stores decrease during lethargus and ATP levels decrease during lethargus and over the course of UV SIS[61]. PRQ may allow the animal to compensate for energy depletion associated with an active response with cessation of locomotion and feeding. However, we consider this energy-based argument unlikely since longer stimuli elicit more activity than brief stimuli without causing PRQ.

A third possibility is that PRQ represents a form of defensive freezing, analogous to the freezing phase in the classic mammalian escape response[3,4]. A cessation of movement can help an animal that has detected a predator to evade detection by the predator[3,7]. Given the limited visibility in *C. elegans*' natural environment of decaying organic material, it is likely that its predators rely on primarily olfactory, mechanosensory, and potentially electrosensory[62] cues rather than visual ones for prey seeking and identification. *C. elegans'* natural predators likely include nematophagous arthropods, fungi, and other nematodes[32,63,64]. PRQ may allow *C. elegans* to avoid detection after retreating from contact with a predator by minimizing mechanosensory stimulation, electromyogenic cues, and potentially olfactory cues, since touch suppresses defecation[65]. Reduced feeding during PRQ (and after touch generally) may help minimize the ingestion of harmful fungal or bacterial spores, and the suppression of head

movement during PRQ suggests it may be related to the tyramine-dependent suppression of head movement during *C. elegans* escape behavior[32,54].

Additional lines of evidence support an association between PRQ and defensive behaviors. We found that RIS function is required for PRQ, and *unc-25* (GABA synthesis) mutants show a partial deficit in PRQ. GABAergic function in the RIS neuron has been found to regulate C. elegans avoidance of kairomones released by the predatory nematode *Pristionchus pacificus*[66], supporting a connection between PRQ and defensive avoidance behavior. We also found that PRQ depends on EGF signaling. In mice, the EGF-family receptor neuregulin-1 has been shown to modulate anxiety-like behaviors[67,68]; for example, overexpression of the neuregulin-1 receptor increases baseline startle response[69]. These results suggest that EGF family signaling may play conserved roles in regulating defensive and fear/anxiety behaviors.

In summary, PRQ represents a novel feature of *C. elegans* escape behavior during a stress state. Further study of its circuit and genetic bases will enrich our understanding of the mechanisms modulating animal responses to aversive stimuli.

Methods

C. elegans strains & maintenance

We cultured *C. elegans* on OP50 *E. coli* food bacteria on standard NGM agar plates[36] at 20°C, and experiments were performed at ambient lab temperature, which ranged 18°C – 24°C. Unless otherwise specified, we performed experiments using young adult hermaphrodites staged by picking late L4s 5 – 7 hours prior to the experiment. The exceptions to this are the lethargus experiments, where we used mid to late L4s picked just before the experiment.

Strains used in this study and the phenotypes used for identifying mutant progeny are given in Table 1. We used the Bristol N2 strain as wild-type. For EGF overexpression experiments in a wild-type background, we crossed PS5009 *pha-1(e2132ts)* III.; *him-5(e1490)* V. syEx723[*hsp16-41*::*lin-3c*; *myo-2*:GFP; *pha-1*(+)][13] with N2 to make YX256. For EGF overexpression experiments in other mutant backgrounds, we crossed mutant strains with YX256 males to generate strains carrying *syEx723* in the mutant background. We used the phenotype indicated in the chart below to identify mutant progeny. All mutants used to generate crosses are available from the CGC.

Strain	**Genotype**	**Phenotype**	**Origin**
Bristol N2	WT		
YX256	*syEx723* [*hsp16-41*::*lin-3c*; *myo-2*:GFP; *pha-1(+)*]	-	PS5009 x N2
YX270	*npr-1(ad609)* X; syEx723	Clumping	YX256 x

			DA609
YX271	*unc-31(e928)* IV; syEx723	Uncoordinated	YX256 x DA509
YX272	*unc-7(e5)* X; syEx723	Uncoordinated	YX256 x CB5
YX273	*daf-16(mu86)* I; syEx723	Reduced paraquat resistance[34]	YX256 x CF1038
YX276	*aptf-1 (tm3287)* II; syEx723	Reduced lethargus quiescence	YX256 x HBR232
YX277	*ceh-17 (np1)* I; syEx723	Reduced UV SIS quiescence	YX256 x IB16
YX278	*unc-25*(e156) III; syEx723	Uncoordinated	YX256 x CB156
YX280	*unc-31(e169)* IV; syEx723	Uncoordinated	YX256 x CB169
YX281	*ceh-14(ch3)* X; syEx723	Reduced UV SIS quiescence	YX256 x TB528
YX282	*mec-4(u253)* X; syEx723	Mechanosensory defect	YX256 x TU253

Table 1. Strains used in this study and the phenotypes used for identifying mutants.

Heat shock, UV, and other stressors

UV: To expose worms in WorMotels to UV light, we used a Spectrolinker XL-1000 UV Crosslinker (Spectronics Corporation, Westbury, NY) with UV-C (254 nm) fluorescent tubes. The WorMotel was placed uncovered on a flat black background in the bottom middle of the crosslinker, and the crosslinker was run at the indicated energy dose from a cold start (after having been off for at least several hours).

Heat: For most experiments, we used a thermal immersion circulator to maintain a water bath at the specified temperature. For some experiments, we used a hot plate and added hot or cold water to maintain the temperature. We fully immersed a Parafilmed petri dish containing the WorMotel for the specified time, then placed the petri dish on the lab bench for about 5 min to return to ambient temperature before proceeding.

Cold: We chilled a Parafilm-sealed petri dish containing the WorMotel and young adult worms in a 4°C refrigerator or 4°C thermal circulator for 24 hours.

Salt: We picked WT worms from a WorMotel into NGMB (NGM buffer) containing an additional 500 mM NaCl for 15 minutes and then picked them back onto the WorMotel using an eyebrow pick. Controls for this experiment were picked into regular NGMB without extra salt. NGMB has the same composition as Nematode Growth Medium (NGM)[70] but without agar, peptone, or

cholesterol.

Ethanol: We picked WT worms from a WorMotel into a 5% (v/v) solution of ethanol in NGMB for 15 minutes using an eyebrow hair pick. Controls for this experiment were picked into regular NGMB without ethanol.

Cry5b: We transferred WT worms from the WorMotel onto a standard NGM plate seeded with Cry5b-expressing bacteria[14,71] and left the animals on the Cry5b-expressing bacteria for 15 minutes and then transferred them back onto individual wells of the WorMotel. Controls were picked onto a plate seeded with bacteria expressing the vector backbone of the Cry5b-expressing plasmids.

Mechanosensory stimulation

For mechanosensory assays performed while imaging using dark field illumination, we coupled the WorMotel to an audio loudspeaker (PLMRW10 10-Inch Marine Subwoofer, Pyle Audio Inc., Brooklyn, NY). Acrylic mounting plates with screws fixed the WorMotel tightly to the inside of a 10 cm petri dish, which itself was mounted on the center of the speaker cone using an acrylic ring and screws. The field was illuminated with a ring of red LEDs situated around the Petri dish.

For mechanostimulus assays performed with bright field imaging for scoring pharyngeal pumps, we coupled a 3 mm thick agar pad contained in a custom acrylic pad holder to a BOSS BRS40 4-inch audio loudspeaker (BOSS Audio Systems, Oxnard, CA) using a 50 mL polystyrene pipette tip glued to the middle of the speaker cone and projecting horizontally. A notch was cut into the end of the pipette tip to fit snugly onto a tab on the pad holder, transferring vibrations from the speaker to the worm substrate.

For all mechanosensory assays, we used a custom MATLAB script to output audio signals though either a NIDAQ PCI-6281 (National Instruments, Austin, TX) or the computer's audio jack to a KAC-M1804 Amplifier (Kenwood, Long Beach, CA), which powered the loudspeaker. Audio signals from the NIDAQ were 1 kHz at a 1 V 0 to peak amplitude except where noted. The beginning and end of the envelope of the audio waveform were made smooth by initiating and terminating using two halves of a 0.1 second Hann window. Waveform duration varied by experiment as specified.

Blue light stimulation

The blue light setup is similar to one previously described[34]. We used a high power blue LED (Luminus PT-121, Sunnyvale, CA, center wavelength 461 nm) driven at 20 A using a DC power supply to illuminate the worms with 0.36 mW / mm^2 blue light. To improve illumination

uniformity, we placed the WorMotel and LED inside a box made of mirrored acrylic interior walls. A custom MATLAB script controlled illumination timing through a NIDAQ USB6001 (National Instruments, Austin, TX) data input/output device and relay (6325AXXMDS-DC3, Schneider Electric, France).

WorMotel fabrication and preparation

We fabricated WorMotels as described previously[34]. Briefly, we poured PDMS (Dow Corning Sylgard 184) into 3D-printed acrylic or polycarbonate molds, cured them overnight at 50 °C, and then removed the PDMS WorMotel devices. We boiled WorMotels in DI water to sanitize them, baked them in a 50°C oven to dry, and treated them with oxygen plasma for 10 seconds in a plasma oven consisting of a Plasma Preen II 973 controller (Plasmatic Systems, Inc.) connected to a microwave oven (Amana RCS10TS). Plasma treatment makes the PDMS device hydrophilic, rendering it easier to fill and the agar surfaces flatter.

We used a pipette to fill the wells with either media containing 3 g/L low melt agarose (Research Products International, Mount Prospect, IL), 5 mg / L cholesterol, 2.5 mg / L bacto-peptone, 1 mM $CaCl_2$, 1 mM $MgSO_4$, 20 mM KH_2PO_4, and 5mM K_2HPO_4) (variable duration blue light and vibration experiments) or standard NGM agar[36] (all other experiments). To reduce the rate of worms escaping from their wells, we filled the moats surrounding the wells with an aversive solution of 100 mM $CuSO_4$[34].

We seeded agarose-filled WorMotels with 5 µL of an overnight *E. coli* OP50 culture resuspended in 3g / L NaCl and allowed the bacteria to dry, re-wetting faster drying wells with DI water to ensure even drying overall, and either used the WorMotels immediately or stored them in a Parafilmed dish with hydrated water crystals (AGSAP PAM, small particle size, M2 Polymer, 1.5 g in 500 mL water) at 4°C for up to two weeks. We seeded agar-filled WorMotels with 2 µL of an overnight culture of OP50 in LB, and aspirated excess LB before allowing the WorMotels to dry open in a biosafety cabinet for 8 minutes. We incubated these WorMotels in a Parafilmed dish with hydrated water crystals (150:1 water:crystals) at 20°C, allowing a bacterial lawn to grow for three days. We either used them immediately or stored them at 4°C for up to two weeks until needed.

After each experiment, we emptied the wells of agar / agarose, washed the WorMotels with hot water and detergent (Alconox), rinsed in DI water, dried, and stored them for reuse.

Imaging and image processing in the WorMotel

For imaging in the WorMotel, we used a 10.7 MP CMOS camera (DMK 24UJ003, The Imaging Source, Charlotte, NC) and 12.5 mm lens (HF12.5SA-1, Fujifilm Corp., Tokyo, Japan) controlled by MATLAB (MathWorks, Natick, MA) to acquire 8 bit, 10 MP grayscale images of

worms in WorMotel wells at 1 frame per second. Red (wavelength 628 nm) LED strips (Oznium, Pagosa Spring, CO) provided dark field illumination. For most experiments, we imaged 24 wells (a 4 x 6 array) at resolution of approximately 7.4 μm per pixel. The exceptions to this were data used in bout correlation analysis, where we used the same camera with a 50 mm lens (Fujinon HF50SA-1, Fujifilm Corp., Tokyo, Japan) to image 6 wells (2 x 3 array) at approximately 280 pixels / mm for L4 lethargus or 12 wells (3 x 4 array) at approximately 200 pixels / mm for young adult SIS and EGF-induced quiescence.

We used custom MATLAB scripts for image processing. We smoothed consecutive frames with a Gaussian filter ($\sigma = 1.5$ pixels) and then subtracted them. We binarized the absolute value of the resulting difference image using a grayscale threshold value of 5. The number of non-zero pixels in each binarized difference image was summed to determine the activity of each worm. A worm was considered quiescent if no activity was detected in its well region of interest for one frame, and active otherwise. The only exception was for bout correlation analysis, where we used a 2 second floor on quiescent bouts in keeping with the literature[51,52]. To calculate normalized activity for each worm, we divided the activity value of each frame pair by the average activity from 50 most active frames after excluding the top 0.5%. Stimulus frames and stimulus-adjacent frames were excluded from analysis, as were wells containing no worms, more than one worm, or in which the worm escaped the well or burrowed into the substrate during recording. Four worms that remained immobile and non-responsive for the entire recording period following cold shock were also censored.

Quantification of stimulus response

Responsiveness was calculated by first averaging the activity of each animal over stimuli in the concerned time period, and then finding the mean activity for five seconds following the stimulus (starting after the stimulus and stimulus adjacent frame), and subtracting the average activity in the minute prior to the stimulus (again, excluding the stimulus frame and the frame before it). Responses were normalized to those of controls (untreated in UV SIS experiments or WT in EGF overexpression experiments) when examining how SIS and EGF overexpression affect arousability. For quantifying the responses of *unc-31* animals and their controls, activity was first calculated by subtraction of non-consecutive frames separated by five seconds, and activity resulting from movement during the stimulus minus baseline activity was used as a measure of the response **(Supplementary Fig. S5,6)**.

Quantification of PRQ

PRQ was calculated by first taking the average quiescence of each animal before and after stimuli in the time period of interest, smoothing this trace with a 10 second window averaging filter, and then subtracting the highest quiescence level in any 10 second period in the two minutes before the stimulus from the highest quiescence level in any 10 second period

in the two minutes after the stimulus. The only exception was for comparison of quiescent bout-interrupted PRQ to active bout-interrupted PRQ **(Fig. 5d)**, where the baseline period was shifted by two minutes earlier to avoid the increase or decrease in quiescence leading up to the stimulus in the two groups, respectively.

Imaging and scoring locomotion, head movement, and feeding

To image pharyngeal pumping, we manually tracked unconstrained worms on an agar pad containing OP50 bacteria using an M156 FC stereo microscope (Leica, Wetzlar, Germany) with a 1.0X Plan Apo objective and white, bright field illumination. We used a 5 MP CMOS camera (DMK33GP031, The Imaging Source, Charlotte, NC) to image at 50 fps with a resolution of approximately 700 pixels / mm and a field of view of approximately 0.91 mm x 0.68 mm.

We used custom MATLAB graphical user interfaces to replay images at approximately 15 fps and score individual pumps, the locomotion state (forward, pause, or backward relative to the substrate), and the head motion state (active or quiescent) of the worm from 30 s before the stimulus to 60 s afterward, censoring frames where the behavior could not be scored with confidence. The scorer was blind to which group the worm belonged to (pre- or 1-6 h post-EGF overexpression).

Lifespan measurements

For lifespan measurements, WorMotels were filled with NGM agar as described, except the agar contained 200 μM fluoro-2'-deoxyuridine (FUdR) to inhibit reproduction, and the WorMotels were seeded with 5 μL of a concentrated suspension of OP50 *E. coli*, which was allowed to partially dry to eliminate liquid on the agar surface. We picked late L4 hermaphrodites into the WorMotel wells, and then treated the UV group as described above. We scored the worms manually on the days noted. A worm was considered dead if it was not moving or feeding spontaneously and failed to respond to a prod with a platinum wire pick.

Statistics

All statistical tests were performed in MATLAB. Statistical tests and p-values used are listed in the figure captions. The Anderson-Darling test was used to test for normality. If any dataset in a set of related experiments was found to be non-normal, we used non-parametric statistical tests for comparisons.

Acknowledgements

We thank Raffi Aroian for Cry5b, Paul Sternberg for strain PS5009, and Martin Chalfie and Matthew Kayser for helpful discussions. Some strains were provided by the CGC, which is funded by NIH Office of Research Infrastructure Programs (P40 OD010440).

References

1. Kleitman, N. Sleep. *Physiol. Rev.* **9**, 624–665 (1929).
2. Heller, H. C. Hibernation: neural aspects. *Annu. Rev. Physiol.* **41**, 305–321 (1979).
3. Roelofs, K. Freeze for action: Neurobiological mechanisms in animal and human freezing. *Philos. Trans. R. Soc. B* **372**, (2017).
4. Bracha, H. S. Freeze, Flight, Fight, Fright, Faint: Adaptationist Perspectives on the Acute Stress Response Spectrum. *CNS Spectr.* **9**, 679–685 (2004).
5. Ratner. Comparative Aspects of Animal Hypnosis. in *Handbook of clinical and experimental hypnosis.* (1967).
6. Cannon, W. B. *Bodily Changes in Fear, Hunger, Pain, and Rage*. (1916).
7. Sargeant, A. B. & Eberhardt, L. E. Death Feigning by Ducks in Response to Predation by Red Foxes. *Am. Midl. Nat.* **94**, 108–119 (1975).
8. Selye, H. The General-Adaptation-Syndrome. *Annu. Rev. Med.* **2**, 327–342 (1951).
9. Selye, H. A syndrome produced by diverse nocuous agents. *Nature* **1936**, 32 (1936).
10. Koolhaas, J. M. *et al.* Coping styles in animals: current status in behavior and stress-psychology. *Neurosci. Biobehav. Rev.* **23**, 925–935 (1999).
11. Rau, V., DeCola, J. P. & Fanselow, M. S. Stress-induced enhancement of fear learning: An animal model of posttraumatic stress disorder. *Neurosci. Biobehav. Rev.* **29**, 1207–1223 (2005).
12. Perusini, J. N. & Fanselow, M. S. Neurobehavioral perspectives on the distinction between fear and anxiety. *Learn. Mem.* **22**, 417–425 (2015).
13. Van Buskirk, C. & Sternberg, P. W. Epidermal growth factor signaling induces behavioral quiescence in Caenorhabditis elegans. *Nat. Neurosci.* **10**, 1300–1307 (2007).
14. Hill, A. J., Mansfield, R., Lopez, J. M. N. G., Raizen, D. M. & Van Buskirk, C. Cellular stress induces a protective sleep-like state in C. elegans. *Curr. Biol.* **24**, 2399–2405 (2014).
15. Fry, A. L., Laboy, J. T., Huang, H., Hart, A. C. & Norman, K. R. A conserved GEF for Rho-family GTPases acts in an EGF signaling pathway to promote sleep-like quiescence in Caenorhabditis elegans. *Genetics* **202**, 1153–1166 (2016).
16. Konietzka, J. *et al.* Epidermal Growth Factor signaling acts directly and through a sedation neuron to depolarizes a sleep-active neuron following cellular stress. *bioRxiv* (2019). doi:http://dx.doi.org/10.1101/656512
17. Nelson, M. D. *et al.* FMRFamide-like FLP-13 Neuropeptides Promote Quiescence following Heat Stress in Caenorhabditis elegans. *Curr. Biol.* **24**, 1–5 (2014).
18. Nath, R. D., Chow, E. S., Wang, H., Schwarz, E. M. & Sternberg, P. W. C. elegans Stress-Induced Sleep Emerges from the Collective Action of Multiple Neuropeptides. *Curr. Biol.* **26**, 2446–2455 (2016).
19. Cho, J. Y. & Sternberg, P. W. Multilevel Modulation of a Sensory Motor Circuit During C. elegans Sleep and Arousal. *Cell* **156**, 249–260 (2014).
20. Trojanowski, N. F. & Raizen, D. M. Call it Worm Sleep. *Trends Neurosci.* **39**, 54–62 (2016).
21. Kushikata, T., Fang, J., Chen, Z., Wang, Y. & Krueger, J. M. Epidermal growth factor enhances spontaneous sleep in rabbits. *Am. J. Physiol.* **275**, R509-14 (1998).
22. Kramer, A. *et al.* Regulation of daily locomotor activity and sleep by hypothalamic EGF receptor signating. *Science (80-.).* **294**, 2511–2515 (2001).

23. Konturek, S. J., Brzozowski, T., Konturek, P. K., Majka, J. & Dembiński, A. Role of salivary glands and epidermal growth factor (EGF) in gastric secretion and mucosal integrity in rats exposed to stress. *Regul. Pept.* **32**, 203–215 (1991).
24. Chalfie, M. & Sulston, J. Developmental Genetics of the Mechanosensory Neurons of Caenorhabditis elegans. *Dev. Biol.* **82**, 358–370 (1981).
25. Chalfie, M. *et al.* The neural circuit for touch sensitivity in Caenorhabditis elegans. *J. Neurosci.* **5**, 956–64 (1985).
26. Bargmann, C. I., Thomas, J. H. & Horvitz, H. R. Chemosensory cell function in the behavior and development of Caenorhabditis elegans. *Cold Spring Harb. Symp. Quant. Biol.* **55**, 529–538 (1990).
27. Culotti, J. G. & Russell, R. L. Osmotic avoidance defective mutants of the nematode Caenorhabditis elegans. *Genetics* **90**, 243–256 (1978).
28. Edwards, S. L. *et al.* A novel molecular solution for ultraviolet light detection in Caenorhabditis elegans. *PLoS Biol.* **6**, 1715–1729 (2008).
29. Wittenburg, N. & Baumeister, R. Thermal avoidance in Caenorhabditis elegans: An approach to the study of nociception. *Proc. Natl. Acad. Sci.* **96**, 10477–10482 (1999).
30. Roeder, T., Seifert, M., Kähler, C. & Gewecke, M. Tyramine and octopamine: Antagonistic modulators of behavior and metabolism. *Arch. Insect Biochem. Physiol.* **54**, 1–13 (2003).
31. Alkema, M. J., Hunter-Ensor, M., Ringstad, N. & Horvitz, H. R. Tyramine functions independently of octopamine in the Caenorhabditis elegans nervous system. *Neuron* **46**, 247–260 (2005).
32. Maguire, S. M., Clark, C. M., Nunnari, J., Pirri, J. K. & Alkema, M. J. The C. elegans touch response facilitates escape from predacious fungi. *Curr. Biol.* **21**, 1326–30 (2011).
33. DeBardeleben, H. K., Lopes, L. E., Nessel, M. P. & Raizen, D. M. Stress-Induced Sleep After Exposure to Ultraviolet Light is Promoted by p53 in Caenorhabditis elegans. *Genetics* **207**, 571–582 (2017).
34. Churgin, M. A. *et al.* Longitudinal imaging of Caenorhabditis elegans in a microfabricated device reveals variation in behavioral decline during aging. *Elife* **6**, 1–25 (2017).
35. Raizen, D. M. *et al.* Lethargus is a Caenorhabditis elegans sleep-like state. *Nature* **451**, 569–72 (2008).
36. Brenner, S. The Genetics of Caenorhabditis elegans. *Genetics* **77**, 71–94 (1974).
37. Rankin, C. H., Beck, C. D. & Chiba, C. M. Caenorhabditis elegans: a new model system for the study of learning and memory. *Behav. Brain Res.* **37**, 89–92 (1990).
38. Schwarz, J., Lewandrowski, I. & Bringmann, H. Reduced activity of a sensory neuron during a sleep-like state in Caenorhabditis elegans. *Curr. Biol.* **21**, R983–R984 (2011).
39. Singh, K., Ju, J. Y., Walsh, M. B., DiIorio, M. A. & Hart, A. C. Deep conservation of Genes Required for Both Drosphila melanogaster and Caenorhabditis elegans Sleep Includes a Role for Dopaminergic Signaling. *Sleep* **37**, 1439–51 (2014).
40. Turek, M., Lewandrowski, I. & Bringmann, H. An AP2 transcription factor is required for a sleep-active neuron to induce sleep-like quiescence in C. elegans. *Curr. Biol.* **23**, 2215–2223 (2013).
41. Van Buskirk, C. & Sternberg, P. W. Paired and LIM class homeodomain proteins coordinate differentiation of the C. elegans ALA neuron. *Development* **137**, 2065–2074 (2010).
42. Turek, M., Besseling, J., Spies, J., Konig, S. & Bringmann, H. Sleep-active neuron specification and sleep induction require FLP-11 neuropeptides to systemically induce sleep. *Elife* **5**, 1–18 (2016).
43. Wu, Y., Masurat, F., Preis, J. & Bringmann, H. Sleep Counteracts Aging Phenotypes to Survive Starvation-Induced Developmental Arrest in C. elegans. *Curr. Biol.* **28**, 1–14 (2018).
44. Nelson, M. D. *et al.* The neuropeptide NLP-22 regulates a sleep-like state in Caenorhabditis elegans. *Nat. Commun.* **4**, 2846 (2013).
45. Jacob, T. C. & Kaplan, J. M. The EGL-21 Carboxypeptidase E Facilitates Acetylcholine

Release at Caenorhabditis elegans Neuromuscular Junctions. *J. Neurosci.* **23**, 2122–2130 (2003).
46. Sieburth, D. *et al.* Systematic analysis of genes required for synapse structure and function. *Nature* **436**, 510–516 (2005).
47. Avery, L., Bargmann, C. I. & Horvitz, H. R. The Caenorhabditis elegans unc-31 Gene Affects Multiple Nervous System-Controlled Functions. *Genetics* **134**, 455–464 (1993).
48. McIntire, S. L., Jorgensen, E., Kaplan, J. & Horvitz, H. R. The GABAergic nervous system of C.elegans. *Nature* **364**, 337–341 (1993).
49. Jin, Y., Jorgensen, E., Hartwieg, E. & Horvitz, H. R. The Caenorhabditis elegans Gene unc-25 Encodes Glutamic Acid Decarboxylase and Is Required for Synaptic Transmission But Not Synaptic Development. *J. Neurosci.* **19**, 539–548 (1999).
50. Borbély, A. A. A Two Process Model of Sleep Regulation. *Hum. Neurobiol.* **1**, 195–204 (1982).
51. Iwanir, S. *et al.* The Microarchitecture of C . elegans Behavior during Lethargus : Homeostatic Bout Dynamics , a Typical Body Posture , and Regulation by a Central Neuron. *Sleep* **36**, 385–395 (2013).
52. Nagy, S. *et al.* Homeostasis in C. elegans sleep is characterized by two behaviorally and genetically distinct mechanisms. *Elife* **3**, 1–21 (2014).
53. Driver, R. J., Lamb, A. L., Wyner, A. J. & Raizen, D. M. DAF-16/FOXO regulates homeostasis of essential sleep-like behavior during larval transitions in C. elegans. *Curr. Biol.* **23**, 501–506 (2013).
54. Pirri, J. K. & Alkema, M. J. The neuroethology of C. elegans escape. *Curr. Opin. Neurobiol.* **22**, 187–93 (2012).
55. Robinson, B., Goetting, D. L., Desir, J. C. & Buskirk, C. Van. aptf-1 mutants are primarily defective in head movement quiescence during C . elegans sleep. *micorPublication Biol.* **17**, 17–19 (2019).
56. Hart, A. Behavior. *WormBook* 1–67 (2006). doi:10.1895/wormbook.1.87.1
57. Keane, J. & Avery, L. Mechanosensory inputs influence Caenorhabditis elegans pharyngeal activity via ivermectin sensitivity genes. *Genetics* **164**, 153–162 (2003).
58. Chalfie, M., Hart, A. C., Rankin, C. H. & Goodman, M. B. Assaying mechanosensation. *WormBook* (2014). doi:10.1895/wormbook.1.172.1
59. Gonzales, D. Satiety, Thermosensation and Mechanosensation Regulate a Spontaneous C. elegans Sleep State. 1–38 (2019). doi:10.1101/547075
60. Laranjeiro, R., Harinath, G., Burke, D., Braeckman, B. P. & Driscoll, M. Single swim sessions in C. elegans induce key features of mammalian exercise. *BMC Biol.* **15**, (2017).
61. Grubbs, J. J., Lopes, L. E., Linden, A. M. Van Der & David, M. A salt-induced kinase (SIK) is required for the metabolic regulation of. (2019).
62. Gabel, C. V. *et al.* Neural Circuits Mediate Electrosensory Behavior in Caenorhabditis elegans. *J. Neurosci.* **27**, 7586–7596 (2007).
63. Frézal, L. & Félix, M. A. C. elegans outside the Petri dish. *Elife* **2015**, 1–14 (2015).
64. Schulenburg, H. & Félix, M.-A. The Natural Biotic Environment of Caenorhabditis elegans. *Genetics* **206**, 55–86 (2017).
65. Liu, D. & Thomas, J. Regulation of a periodic motor program in C. elegans. *J. Neurosci.* **14**, 1953–1962 (1994).
66. Liu, Z. *et al.* Predator-secreted sulfolipids induce defensive responses in C. elegans. *Nat. Commun.* **9**, (2018).
67. Bi, L. L. *et al.* Amygdala NRG1-ErbB4 is critical for the modulation of anxiety-like behaviors. *Neuropsychopharmacology* **40**, 974–986 (2015).
68. Karl, T., Duffy, L., Scimone, A., Harvey, R. P. & Schofield, P. R. Altered motor activity, exploration and anxiety in heterozygous neuregulin 1 mutant mice: Implications for understanding schizophrenia. *Genes, Brain Behav.* **6**, 677–687 (2007).
69. Deakin, I. H. *et al.* Behavioural characterization of neuregulin 1 type I overexpressing transgenic mice. *Neuroreport* **20**, 1523–1528 (2009).
70. Stiernagle, T. Maintenance of C. elegans. *WormBook* 1–11 (2006).

doi:10.1895/wormbook.1.101.1
71. Wei, J.-Z. *et al.* Bacillus thuringiensis crystal proteins that target nematodes. *Proc. Natl. Acad. Sci.* **100**, 2760–2765 (2003).

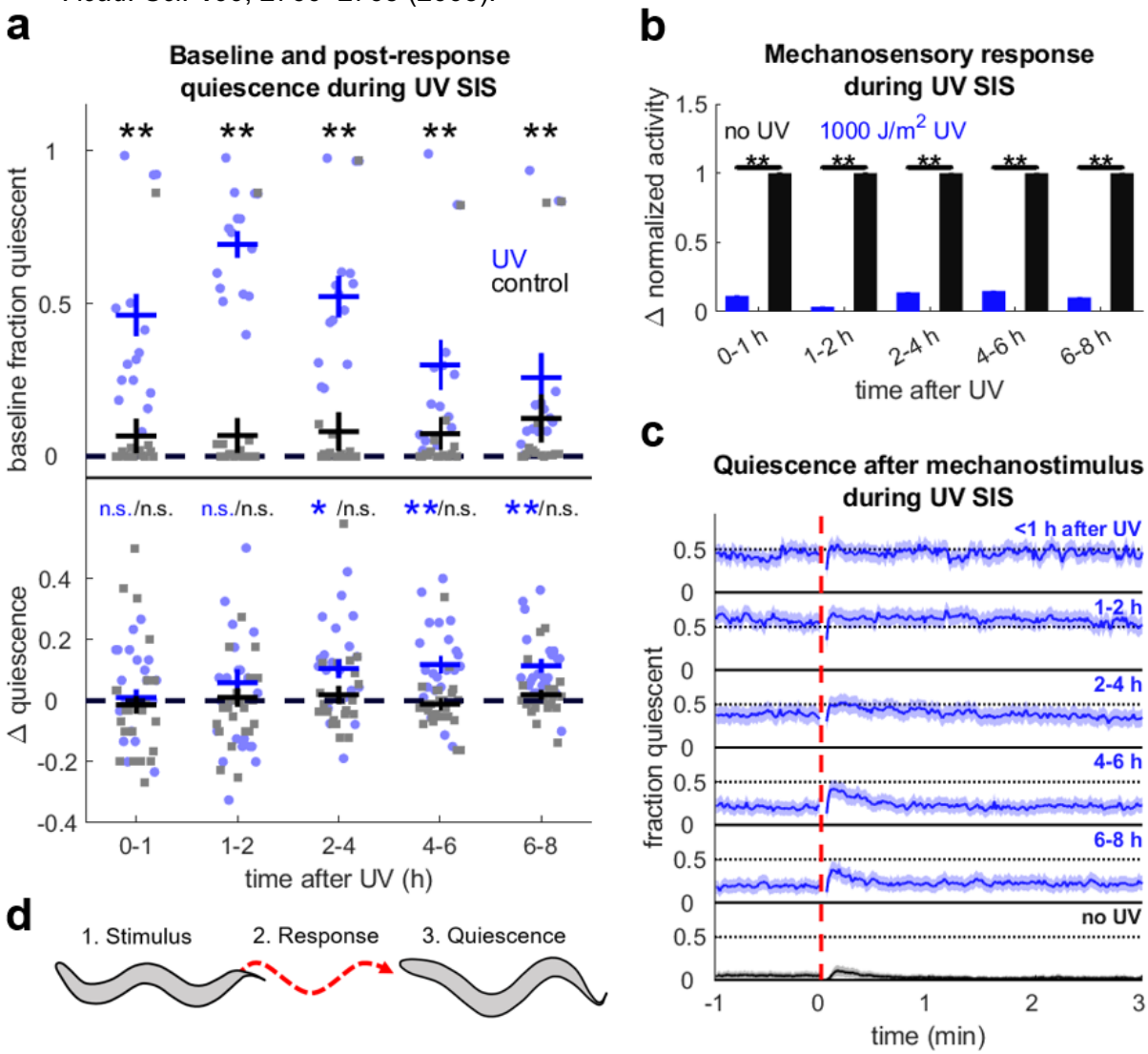

Figure 1. Mechanosensory stimulus during UV SIS elicits post response quiescence.
(a) (top) Average quiescence of WT animals after 1000 J/m^2 UV (blue) and non-exposed controls (black) in the absence of stimuli. Dots represent individual animal averages in 1 or 2 hour bins. n = 15 animals per condition, four replicates. ** denotes $p < 0.01$ comparing UV-treated to controls (Wilcoxon rank-sum test with Bonferroni correction for five comparisons) **(bottom)** Quantification of PRQ. Change in quiescence is the peak quiescence within two minutes after mechanostimulus minus the peak quiescence within two minutes before mechanostimulus in the time bin specified. Typically four or eight responses were averaged per animal and smoothed with a 10 s averaging filter. n = 22 animals per condition, two replicates. ** denotes $p < 0.01$, * denotes $p < 0.05$ (two-sided Wilcoxon signed rank test with Bonferroni correction for five comparisons). Error bars indicate ± SEM.
(b) Mechanosensory response during UV SIS normalized to non-UV controls. Response is the average activity from the five seconds after the stimulus minus the average activity in the minute before the stimulus. The data are from the same animals as panel a (bottom). ** denotes

significance (two-sided Wilcoxon rank-sum test with $\alpha = 0.01$ and Bonferroni correction for five comparisons). Error bars indicate SEM.

(c) Fraction quiescent before and after stimulus (dashed red line) 0-1,1-2, 2-4, 4-6, and 6-8 h (blue) after UV treatment and in non-UV controls averaged throughout the experiment (black). Data are from the same animals as panel a (bottom) and panel b. Shading denotes ± SEM.

(d) Schematic of post-response quiescence: (1) following stimulus, (2) the animal responds by moving, and (3) subsequently becomes quiescent.

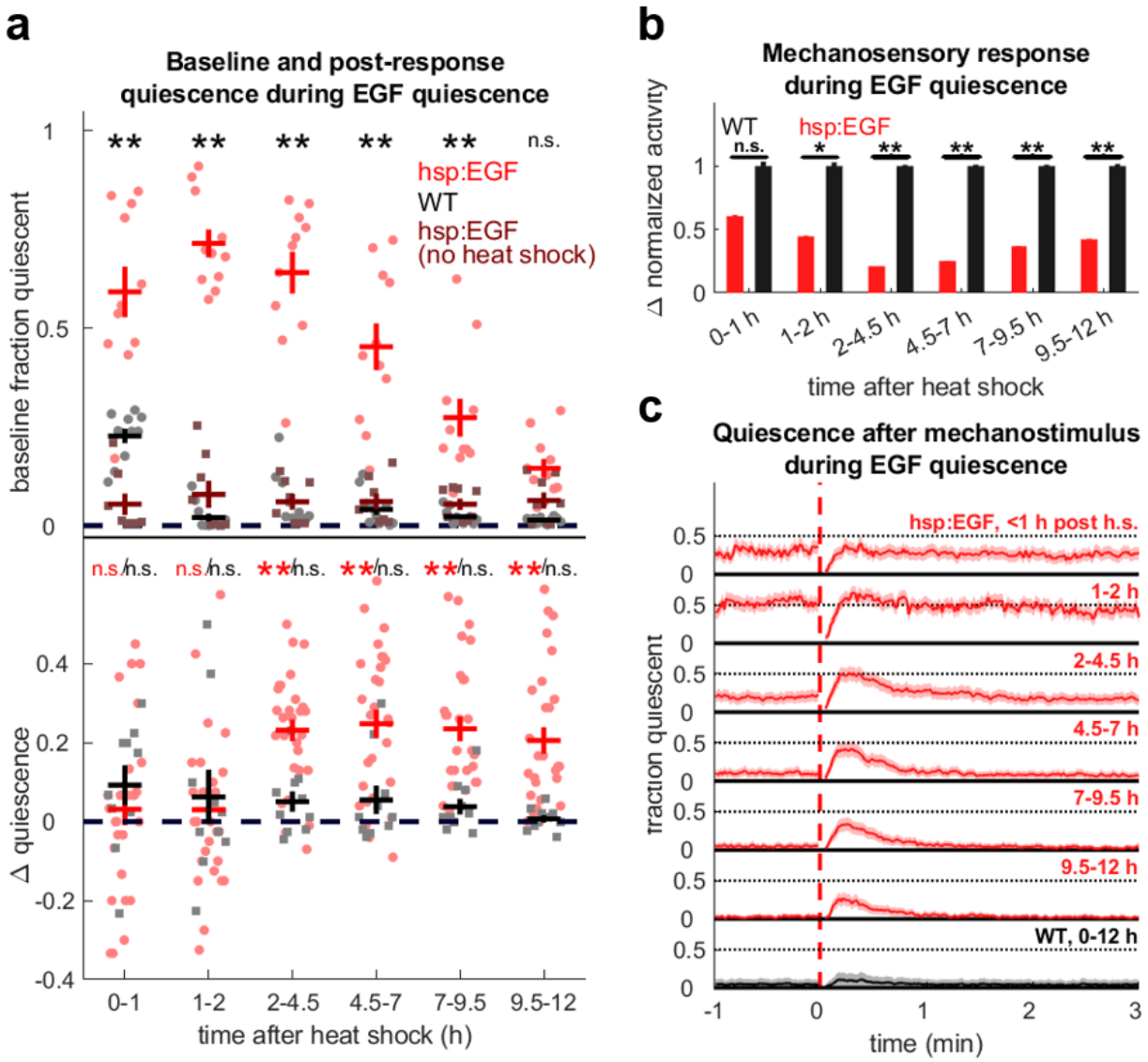

Figure 2. PRQ occurs after EGF overexpression.
(a) (top) Quiescence of hsp:EGF (red, circles) and WT (black, circles) after a mild, 10 min, 32 °C, heat shock and hsp:EGF held at room temperature (burgundy, squares) in the absence of mechanostimulation. n = 8 to 11 animals per condition, two replicates. ** denotes $p < 0.01$ comparing heat shocked hsp:EGF to WT controls (two-sided Wilcoxon rank-sum test with Bonferroni correction for six comparisons) **(bottom)** Quantification of PRQ in hsp:EGF (red) and WT controls (black) after mild heat shock. Change in fraction quiescent was calculated as in Fig. 1a. Pale dots represent individual animal averages. ** denotes $p < 0.01$, two-sided Wilcoxon signed rank test with Bonferroni correction for six comparisons. Error bars indicate ± SEM.
(b) Mechanosensory response after EGF overexpression normalized to mildly heat-shocked WT controls. Response is the average activity from the five seconds after the stimulus minus the average activity in the minute before the stimulus. n = 28, four replicates for hsp:EGF and n = 10, two replicates for WT controls. * denotes $p < 0.05$, ** denotes $p < .01$, two-sided Wilcoxon rank-sum test with Bonferroni correction for six comparisons. Error bars indicate SEM.
(c) Average fraction quiescent before and after stimulus (dashed red vertical line) in hsp:EGF animals 0-1 h,1-2 h, 2-4.5 h, 4.5-7 h, 7-9.5 h, and 9.5-12 h after heat shock (red) and WT animals

0-12 h after heat shock (black). Shading denotes ± SEM. The animals are the same as those in panel b.

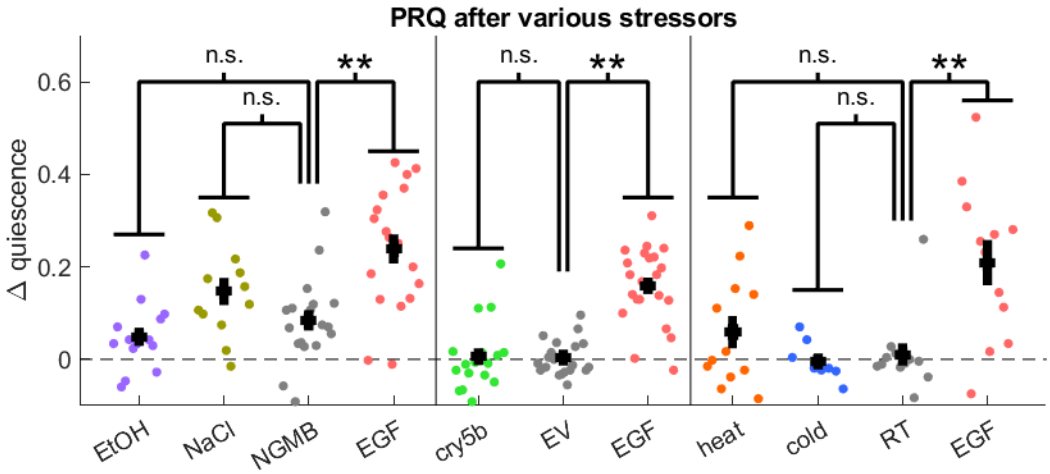

Figure 3. PRQ was not observed in ethanol, high salt, Cry5b toxin, heat, and cold – induced SIS.

PRQ following mechanostimulus after various stressors compared to positive (EGF overexpression, red) and experiment-specific negative controls (gray). **Left**: comparison of PRQ after 15 min immersion in 5% ethanol by volume (purple) or +500 mM NaCl in NGMB (yellow) and EGF overexpression (red) to NGMB-immersed controls (gray). **Middle:** comparison of PRQ in animals after 15 min exposure to Cry5b-expressing bacteria (green) and empty-vector bacteria-exposed animals (gray). **Right:** comparison of PRQ after 30 min, 36°C heat shock (orange) or 24 h, 4°C cold shock (blue) to room temperature controls (gray). Circles are individual animal averages from throughout the experiment (12 h). ** denotes $p < 0.01$ in a two-sided Wilcoxon rank-sum test after Bonferroni correction for three (liquids, left, temperature, right) or two (bacteria toxin, middle) comparisons. Error bars indicate ± SEM.

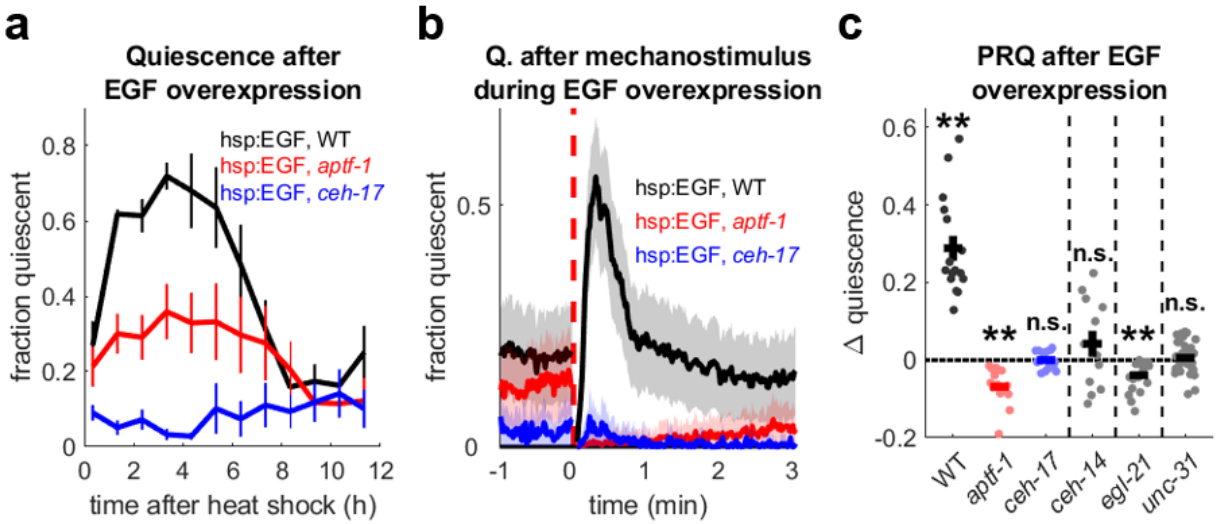

Figure 4. The ALA and RIS neurons and neuropeptide signaling are required for PRQ.
(a) Average quiescence of WT (black) and *apft-1* (red) and *ceh-17* (blue) mutant animals following EGF overexpression in the absence of additional stimuli (quiescence averaged in 1 h bins, n = 8 animals per genotype, one replicate). Error bars represent ± SEM
(b) Fraction quiescent before and after mechanostimulus (vertical dashed red line) in WT (black) and *aptf-1* (red) and *ceh-17* (blue) mutant background animals carrying the hsp:EGF array 2-12 h after mild heat shock. n = 16 animals per genotype, two replicates. Shading represents ± SEM.
(c) (left) Quantification of PRQ in WT and *aptf-1* and *ceh-17* mutants in panel b and **(right)** *ceh-14, egl-21,* and *unc-31* mutants. Dots represent individual animals. ** denotes $p < 0.01$ (two-sided Wilcoxon signed rank test with Bonferroni correction for three comparisons, left, one sample two-tailed t-test, no correction, right). Error bars represent ± SEM

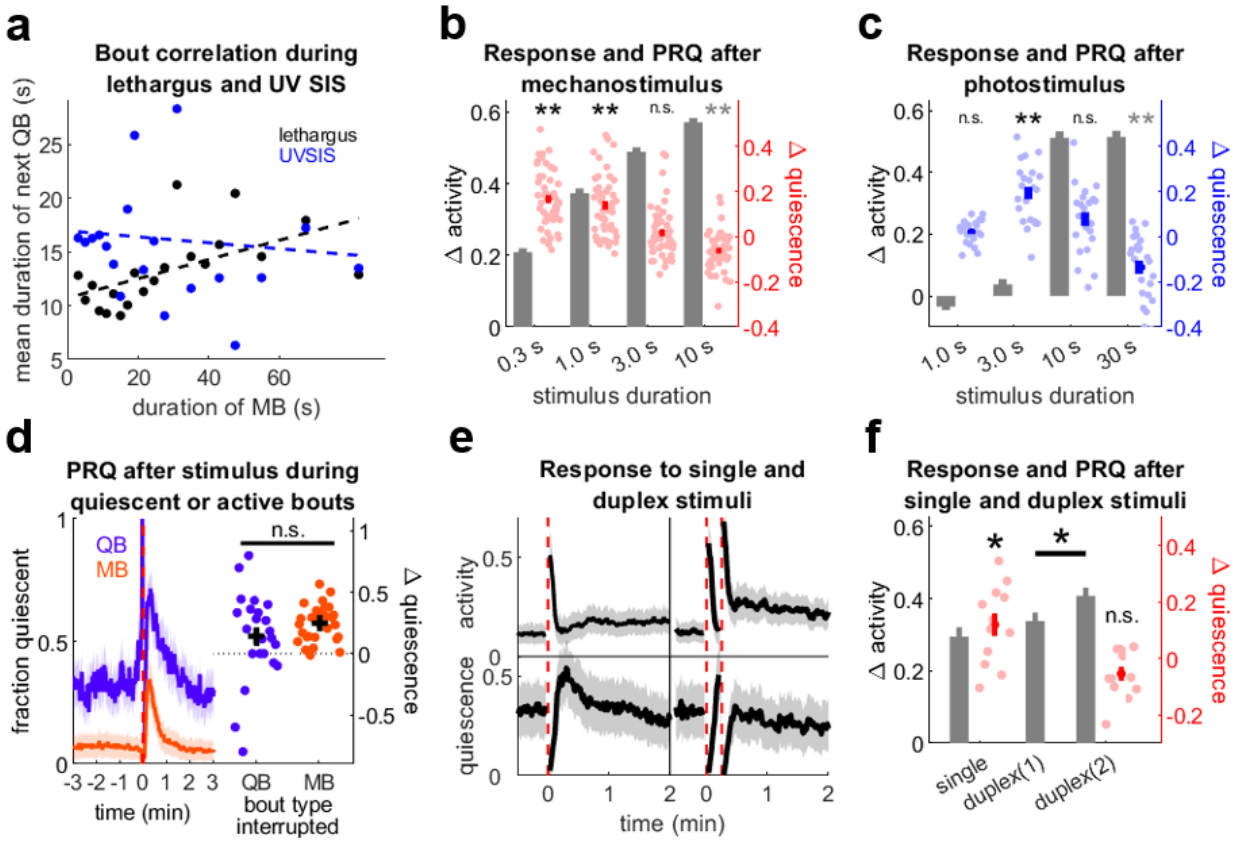

Figure 5. Post-response quiescence lacks the characteristics of sleep homeostasis.
(a) Correlation of the durations of quiescent bouts (QBs) with the preceding movement bout (MB) duration in lethargus (black) and UV SIS (blue). Bout duration was significantly correlated for lethargus (slope = 0.089, p = 0.01, R^2 = 0.32), but not UV SIS (slope = -0.028, p = 0.69, R^2 = 0.0090). n = 17 animals, three replicates for lethargus, n = 12 animals, two replicates for UV SIS.
(b) Mechanosensory response (gray bars) and PRQ (red) of WT background animals 2-12 h after EGF overexpression. ** denotes p < 0.01, two-sided Wilcoxon signed rank test with Bonferroni correction for four comparisons, note that 10 s stimulus animals were *less quiescent* after stimulus. n = 48 animals, four replicates.
(c) Photosensory response (gray bars) and PRQ (blue) of WT background animals 2-12 h after EGF overexpression. ** denotes p < 0.01 (two-sided Wilcoxon signed rank test with Bonferroni correction for four comparisons, note 30 s stimulus animals were *less quiescent* after stimulus). n = 23, two replicates for 1, 3, and 10 s, n = 24, three replicates, for 30 s stimuli)
(d) (left) Average quiescence of WT background animals 2-12 h after EGF overexpression after mechanostimulus when the stimulus interrupted a quiescent bout (blue) or an active bout (red). n = 28 animals, four replicates. These data also appear in figure 2. **(right)** Comparison of PRQ from the left. Data from 4-2 min before the stimulus were used for baseline quiescence. Dots represent single animal averages for stimuli that interrupted quiescent or active bouts. PRQ was not significantly different (p = 0.17, two-tailed, two sample t-test).
(e) Average activity (top) and quiescence (bottom) following a single (left) and duplex (15 s separated) (right) mechanostimuli in WT background animals 2-12 h after EGF overexpression. (n = 12 animals, one replicate). These responses are quantified in panel f.
(f) Mechanosensory response (gray bars) of WT background animals 2-12 h after EGF overexpression after a single and the first and second of a pair of stimuli, and PRQ (red) of the

same animals after single and duplex stimuli. * denotes $p < 0.05$ (one sample t-test with Bonferroni correction for two comparisons or paired sample t-test).
Error bars and shading represent ± SEM.

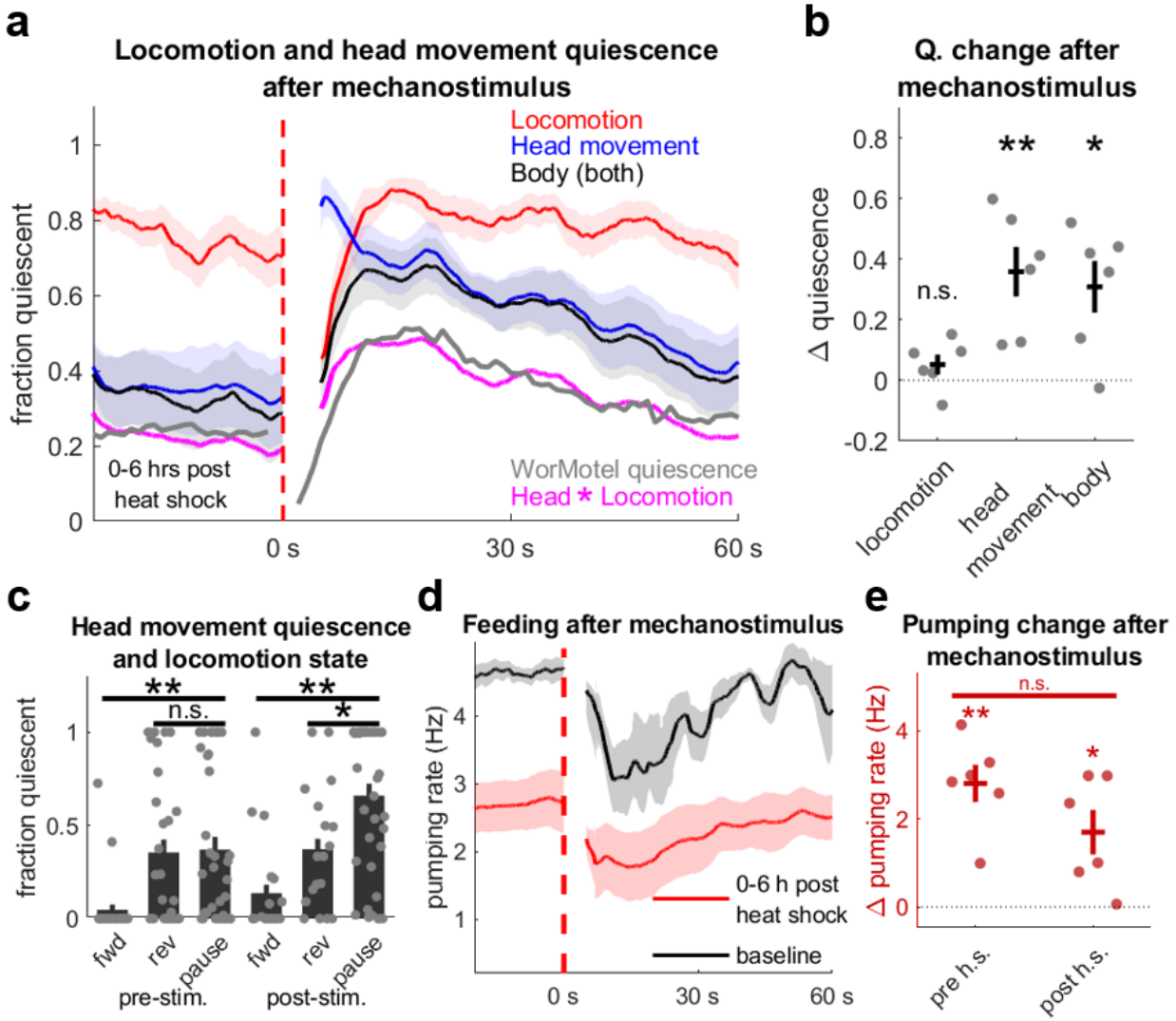

Figure 6. Locomotion, head movement, and feeding during PRQ.

(a) Traces showing fraction of animals locomotion, head movement, and body movement quiescent (both locomotion and head movement quiescent) after mechanostimulus following EGF overexpression. Traces represent the mean of six animals, four recordings each, 0-6 h after heat shock, smoothed with a 5 s window. The magenta trace is the product of the locomotion and head movement traces, and the gray trace is quiescence following mechanostimulus measured in the WorMotel 1-6 hours after EGF overexpression (same data shown in fig. 2b). The dashed red line indicates the stimulus. Data from the same animals are used throughout fig. 6 and supplementary fig. 11.

(b) Average change in peak locomotion, head movement, and body quiescence (black) and average change in minimum pumping rate (red) from the 25 s period before the stimulus to the 25 s period after the stimulus starting at 5 s post stimulus. Circles represent individual animal averages. * denotes $p < 0.05$, ** denotes $p < 0.01$, two-tailed, one sample t-test. Data are the same as panels a-c, 1-6 h post heat shock.

(c) Fraction of time the animals were head movement quiescent while moving forward, reversing, or pausing before (left) and after (right) mechanostimulus. Circles represent single recording averages. * denotes $P < 0.05$, ** denotes $p < 0.01$, two-sided Wilcoxon rank sum test.

(d) Traces showing mean pumping rate before heat shock (black) and 1-6 hours after heat shock (red) after mechanostimulus (dashed line) in hsp:EGF animals. Traces are smoothed with a 5

second averaging window and represent 6 animals, one recording each at prior to heat shock, six recordings each 1-6 hours after heat shock.

(e) Average change in minimum pumping rate from the 25 s period before the stimulus to the 25 s period after the stimulus starting at 5 s post stimulus, before and after heat shock. Circles represent individual animal averages. * denotes $p < 0.05$, ** denotes $p < 0.01$. Two tailed one sample or paired sample t-tests were used. Error bars and shading represent ± SEM.